*Inorg. Chem.* **2007**, *46*, 4049–4059

# Chloro Half-Sandwich Osmium(II) Complexes: Influence of Chelated N,N-Ligands on Hydrolysis, Guanine Binding, and Cytotoxicity

**Anna F. A. Peacock, Abraha Habtemariam, Stephen A. Moggach, Alessandro Prescimone, Simon Parsons, and Peter J. Sadler***

*School of Chemistry, University of Edinburgh, West Mains Road, Edinburgh EH9 3JJ, U.K.*

Received December 8, 2006

Relatively little is known about the kinetics or the pharmacological potential of organometallic complexes of osmium compared to its lighter congeners, iron and ruthenium. We report the synthesis of seven new complexes, $[(\eta^6\text{-arene})Os(NN)Cl]^+$, containing different bidentate nitrogen (N,N) chelators, and a dichlorido complex, $[(\eta^6\text{-arene})Os(N)Cl_2]$. The X-ray crystal structures of seven complexes are reported: $[(\eta^6\text{-bip})Os(en)Cl]PF_6$ (**1PF$_6$**), $[(\eta^6\text{-THA})Os(en)Cl]BF_4$ (**2BF$_4$**), $[(\eta^6\text{-}p\text{-cym})Os(phen)Cl]PF_6$ (**5PF$_6$**), $[(\eta^6\text{-bip})Os(dppz)Cl]PF_6$ (**6PF$_6$**), $[(\eta^6\text{-bip})Os(azpy\text{-}NMe_2)Cl]PF_6$ (**7PF$_6$**), $[(\eta^6\text{-}p\text{-cym})Os(azpy\text{-}NMe_2)Cl]PF_6$ (**8PF$_6$**), and $[(\eta^6\text{-bip})Os(NCCH_3\text{-}N)Cl_2]$ (**9**), where THA = tetrahydroanthracene, en = ethylenediamine, *p*-cym = *p*-cymene, phen = phenanthroline, bip = biphenyl, dppz = [3,2-*a*: 2′,3′-*c*]phenazine and azpy-$NMe_2$ = 4-(2-pyridylazo)-*N*,*N*-dimethylaniline. The chelating ligand was found to play a crucial role in enhancing aqueous stability. The rates of hydrolysis at acidic pH* decreased when the primary amine N-donors (NN = en, $t_{1/2}$ = 0.6 h at 318 K) are replaced with $\pi$-accepting pyridine groups (e.g., NN = phen, $t_{1/2}$ = 9.5 h at 318 K). The $Os^{II}$ complexes hydrolyze up to 100 times more slowly than their $Ru^{II}$ analogues. The $pK_a^*$ of the aqua adducts decreased with a similar trend ($pK_a^*$ = 6.3 and 5.8 for en and phen adducts, respectively). $[(\eta^6\text{-bip})Os(en)Cl]PF_6/BF_4$ (**1PF$_6$/BF$_4$**) and $[(\eta^6\text{-THA})Os(en)Cl]BF_4$ (**2BF$_4$**) were cytotoxic toward both the human A549 lung and A2780 ovarian cancer cell lines, with $IC_{50}$ values of 6–10 $\mu$M, comparable to the anticancer drug carboplatin. **1BF$_4$** binds to both the N7 and phosphate of 5′-GMP (ratio of 2:1). The formation constant for the 9-ethylguanine (9EtG) adduct $[(\eta^6\text{-bip})M(en)(9EtG)]^{2+}$ was lower for $Os^{II}$ (log $K$ = 3.13) than $Ru^{II}$ (log $K$ = 4.78), although the $Os^{II}$ adduct showed some kinetic stability. DNA intercalation of the dppz ligand in **6PF$_6$** may play a role in its cytotoxicity. This work demonstrates that the nature of the chelating ligand can play a crucial role in tuning the chemical and biological properties of $[(\eta^6\text{-arene})Os(NN)Cl]^+$ complexes.

## Introduction

The design and development of organometallic drugs is a relatively new but rapidly developing field.[1,2] Organometallic complexes of the group 8 elements ruthenium and iron are receiving increasing attention as potential anticancer agents,[3−6] yet the pharmacological potential of organometallic osmium complexes has been little explored. In general, not much is known about the chemistry of osmium arene complexes compared to those of iron and ruthenium. A SciFinder search revealed ∼8 times fewer publications on osmium arene complexes.

Ruthenium and platinum complexes containing chelating N,N-heterocyclic ligands, for example, phenanthroline (phen), bipyridine (bipy), and phenylazo-pyridine (azpy), have been extensively studied, and some have been reported to show anticancer activity.[7−9] Romeo et al. investigated the ligand exchange kinetics of platinum complexes containing different

* To whom correspondence should be addressed. E-mail P.J.Sadler@ed.ac.uk.

(1) Fish, R. H.; Jaouen, G. *Organometallics* **2003**, *22*, 2166−2177.
(2) Melchart, M.; Sadler, P. J. In *Bioorganometallics*; Jaouen, G., Ed.; Wiley-VCH: Weinheim, Germany, 2006; Vol. 1, pp 39−64.
(3) Allardyce, C. S.; Dorcier, A.; Scolaro, C.; Dyson, P. J. *Appl. Organomet. Chem.* **2005**, *19*, 1−10.
(4) Yan, Y. K.; Melchart, M.; Habtemariam, A.; Sadler, P. J. *Chem. Comm.* **2005**, 4764−4776.
(5) Hillard, E.; Vessieres, A.; Le, Bideau, F.; Plazuk, D.; Spera, D.; Huche, M.; Jaouen, G. *ChemMedChem.* **2006**, *1*, 551−559.
(6) Hartinger, C. G.; Nazarov, A. A.; Arion, V. B.; Giester, G.; Jakupec, M.; Galanski, M.; Keppler, B. K. *New J. Chem.* **2002**, *26*, 671−673.
(7) Novakova, O.; Kasparkova, J.; Vrana, O.; van Vliet, P. M.; Reedijk, J.; Brabec, V. *Biochemistry* **1995**, *34*, 12369−78.
(8) Bloemink, M. J.; Engelking, H.; Karentzopoulos, S.; Krebs, B.; Reedijk, J. *Inorg. Chem.* **1996**, *35*, 619 − 627.
(9) Velders, A. H.; Kooijman, H.; Spek, A. L.; Haasnoot, J. G.; De Vos, D.; Reedijk, J. *Inorg. Chem.* **2000**, *39*, 2966−2967.

10.1021/ic062350d CCC: $37.00 
Published on Web 04/19/2007

bidentate nitrogen-chelating ligands,[10] and the DNA intercalation ability of platinum and ruthenium complexes containing this class of ligands has also received attention.[11−14] Osmium complexes containing such heterocyclic bidentate nitrogen chelates have been investigated as DNA photoreagents;[15−17] however these complexes were coordinately saturated, containing no exchangeable ligand, and so provided no information on ligand exchange rates on osmium complexes containing different nitrogen chelators. However, it is clear that bidentate nitrogen chelators such as bipy form characteristically stable osmium complexes.[18] This is potentially important for possible anticancer activity, since we have found that dissociation of oxygen-chelating ligands from osmium at micromolar concentrations can deactivate complexes under biological testing conditions.[19,20]

Here, we explore the solid-state structures, kinetics, and solution behavior of $Os^{II}$ arene complexes containing a series of different bidentate nitrogen chelators, including diamines and azopyridines, and attempt to relate this to their activity toward cancer cell lines. This work may also be relevant to the design of new catalysts.

## Experimental Section

**Materials.** $OsCl_3 \cdot nH_2O$ was purchased from Alfa Aesaer; ethylenediamine and 4-(2-pyridylazo)-*N*,*N*-dimethylaniline (azpy-$NMe_2$) were obtained from Sigma-Aldrich. 9-Ethylguanine and guanosine 5′-monophosphate were purchased from Sigma, and ammonium tetrafluoroborate, ammonium hexafluorophosphate, 2-picolylamine (ampy), 2,2′-bipyridine (bipy), 1,10-phenanthroline (phen), and deuterated solvents came from Aldrich. The dimers $[(\eta^6\text{-bip})OsCl_2]_2$, $[(\eta^6\text{-}p\text{-cym})OsCl_2]_2$, $[(\eta^6\text{-THA})OsCl_2]_2$, ligand [3,2-*a*: 2′,3′-*c*]phenazine (dppz), and the ruthenium complex, $[(\eta^6\text{-bip})Ru(en)Cl]PF_6$, were prepared by previously reported procedures.[19,21−24] Ethylenediamine and methanol/ethanol were distilled over sodium and magnesium/iodine, respectively, prior to use.

**Preparation of Complexes.** Complexes **1PF$_6$/BF$_4$−9** were synthesized from the dimer precursor $[(\eta^6\text{-arene})OsCl_2]_2$.

**$[(\eta^6\text{-bip})Os(en)Cl]BF_4$ (1BF$_4$).** A solution of $[(\eta^6\text{-bip})OsCl_2]_2$ (187 mg, 0.22 mmol) in 12 mL of methanol was heated under reflux for 80 min under argon; ethylenediamine (32 $\mu$L, 0.48 mmol) was added, and the reaction mixture was heated under reflux for a further 40 min. The mixture was filtered through a 0.45 $\mu$m pore size filter while still hot. $NH_4BF_4$ (390 mg, ca. 8 mol equiv) was added; the mixture was stirred, and the solvent was removed on a rotary evaporator. Soxlett extraction using dichloromethane was carried out for 5.5 h. The solvent volume was reduced to ∼5 mL, and the sample was stored at 253 K overnight. The yellow microcrystalline product was recovered by filtration, washed with dichloromethane (10 mL) and diethyl ether (10 mL), and air-dried. Yield: 129 mg (54%). Anal. Calcd for $C_{14}ClH_{18}N_2OsBF_4$ (526.79): C, 31.92; H 3.44; N 5.32%. Found: C, 32.05; H, 3.20; N, 5.07%. $^1$H NMR (DMSO-$d_6$): $\delta$ 7.69 (d, 2H, $J$ = 7.2 Hz), 7.49 (t, 2H, $J$ = 7.6 Hz), 7.44 (t, 1H, $J$ = 7.3 Hz), 7.07 (b, 2H), 6.42 (d, 2H, $J$ = 5.7 Hz), 6.13 (t, 1H, $J$ = 5.0 Hz), 6.03 (t, 2H, $J$ = 5.3 Hz), 4.79 (b, 2H), 2.44 (m, 2H), 2.20 (m, 2H).

**$[(\eta^6\text{-bip})Os(en)Cl]PF_6$ (1PF$_6$).** Synthesis was performed in the same manner as for **1BF$_4$**, using $NH_4PF_6$ instead of $NH_4BF_4$. Yield: 139 mg (67%). ESI-MS Calcd for $C_{14}ClH_{18}N_2Os$: $m/z$ 442.1. Found: $m/z$ 441.4. $^1$H NMR (DMSO-$d_6$): $\delta$ 7.69 (d, 2H, $J$ = 7.2 Hz), 7.49 (t, 2H, $J$ = 7.4 Hz), 7.44 (t, 1H, $J$ = 7.3 Hz), 7.07 (b, 2H), 6.42 (d, 2H, $J$ = 5.5 Hz), 6.13 (t, 1H, $J$ = 5.1 Hz), 6.03 (t, 2H, $J$ = 5.4 Hz), 4.80 (b, 2H), 2.45 (m, 2H), 2.20 (m, 2H). Crystals of **1PF$_6$** suitable for X-ray diffraction were obtained by slow evaporation of a dichloromethane solution at ambient temperature.

**$[(\eta^6\text{-THA})Os(en)Cl]BF_4$ (2BF$_4$).** A solution of $[(\eta^6\text{-THA})OsCl_2]_2$ (27.1 mg, 0.03 mmol) in methanol (5 mL) was refluxed for 1.5 h under an argon atmosphere; ethylenediamine (5 $\mu$L, 0.075 mmol) was added, and the reaction mixture was refluxed for a further 40 min. The mixture was filtered through a glass wool plug while still hot. A filtered solution of $NH_4BF_4$ (29 mg, ∼9 mol equiv) in methanol (2 mL) was added; the mixture was stirred, and the solvent was removed in vacuo. Soxlett extraction using dichloromethane was carried out on the solid residue for 6.5 h. The solvent was allowed to evaporate slowly overnight at ambient temperature (∼0.5 mL). The crystalline product was recovered by filtration, washed with diethyl ether (10 mL), and air-dried. Yield: 6.4 mg (19%). Anal. Calcd for $C_{16}ClH_{22}N_2OsBF_4$ (554.82): C, 34.63; H 4.00; N 5.05%. Found: C, 34.33; H, 3.44; N, 4.87%. $^1$H NMR (DMSO-$d_6$): $\delta$ 6.84 (b, 2H), 5.85 (dd, 2H, $J$ = 4.0 and 1.8 Hz), 5.78 (s, 2H), 5.73 (dd, 2H, $J$ = 3.9 and 1.9 Hz), 4.72 (b, 2H), 3.34 (m, 4H, $J$ = 175.1 and 16.4 Hz), 2.65 (s, 4H), 2.45 (m, 2H), 2.19 (m, 2H). Crystals suitable for X-ray diffraction were obtained by slow evaporation of a dichloromethane solution of **2BF$_4$** at ambient temperature.

**$[(\eta^6\text{-}p\text{-cym})Os(ampy)Cl]PF_6$ (3PF$_6$).** 2-Picolylamine (14 $\mu$L, 0.13 mmol) was added to a solution of $[(\eta^6\text{-}p\text{-cym})OsCl_2]_2$ (49.7 mg, 0.06 mmol) in 4 mL of methanol. The reaction mixture was shielded from light and stirred at ambient temperature for 20 h. A filtered solution of $NH_4PF_6$ (100 mg, ∼5 mol equiv) in 2 mL of MeOH was added, and the solvent volume was reduced on a rotary evaporator until a yellow precipitate began to form (∼2 mL). The reaction vessel was stored at 253 K for 2 h. The product was recovered by filtration, washed with methanol (4 mL) and diethyl ether (10 mL), and air-dried. Yield: 60.6 mg (79%). Anal. Calcd for $C_{16}ClH_{22}N_2OsPF_6$ (614.07): C, 31.35; H 3.62; N 4.57%. Found: C, 30.91; H, 3.33; N, 4.60%. $^1$H NMR (MeOD-$d_4$): $\delta$ 9.06 (d, 1H, $J$ = 5.7 Hz), 7.97 (dd, 1H, $J$ = 8.5 and 7.6 Hz), 7.65 (d, 1H, $J$ = 7.9 Hz), 7.48 (dd, 1H, $J$ = 7.6 and 6.6 Hz), 6.09 (d, 1H, $J$ = 5.5 Hz), 6.06 (d, 1H, $J$ = 5.5 Hz), 5.91 (d, 1H, $J$ = 5.5 Hz),


(10) Romeo, R.; Scolaro, L. M.; Nastasi, N.; Arena, G. *Inorg. Chem.* **1996**, *35*, 5087−5096.
(11) Lippard, S. J. *Acc. Chem. Res.* **1978**, *11*, 211−217.
(12) Blasius, R.; Moucheron, C.; Kirsch-De Mesmaeker, A. *Eur. J. Inorg. Chem.* **2004**, *20*, 3971−3979.
(13) Patel, K. K.; Plummer, E. A.; Darwish, M.; Rodger, A.; Hannon, M. J. *J. Inorg. Biochem.* **2002**, *91*, 220−229.
(14) van der Schilden, K.; Garcia, F.; Kooijman, H.; Spek, A. L.; Haasnoot, J. G; Reedijk J. *Angew. Chem., Int. Ed.* **2004**, *43*, 5668−70.
(15) Holmlin, R. E.; Barton, J. K. *Inorg. Chem.* **1995**, *34*, 7−8.
(16) Content, S.; Mesmaeker, A. K.-D. *J. Chem. Soc., Faraday Trans.* **1997**, *93*, 1089−1094.
(17) Mishima, Y.; Motonaka, J.; Ikeda, S. *Anal. Chim. Acta* **1997**, *345*, 45−50.
(18) Dwyer, F. P.; Goodwin, A.; Gyarfas, E. C. *Aust. J. Chem.* **1962**, *16*, 42−50.
(19) Peacock, A. F. A.; Habtemariam, A.; Fernández, R.; Walland, V.; Fabbiani, F. P. A.; Parsons, S.; Aird, R. E.; Jodrell, D. I.; Sadler, P. J. *J. Am. Chem. Soc.* **2006**, *128*, 1739−1748.
(20) Peacock, A. F. A.; Melchart, M.; Deeth, R. J.; Habtemariam, A.; Parsons, S.; Sadler, P. J. *Chem.−Eur. J.* **2007**, *13*, 2601−2613.
(21) Stahl, S.; Werner, H. *Organometallics* **1990**, *9*, 1876−1881.
(22) Chen, H.; Parkinson, J. A.; Parsons, S.; Coxall, R. A.; Gould, R. O.; Sadler, P. J. *J. Am. Chem. Soc* **2002**, *124*, 3064−3082.
(23) Yamada, M.; Tanaka, Y.; Yoshimoto, Y.; Kuroda, S.; Shimao, I. *Bull. Chem. Soc. Jpn.* **1992**, *65*, 1006−1011.
(24) Morris, R. E.; Aird, R. E.; Murdoch, P. d. S.; Chen, H.; Cummings, J.; Hughes, N. D.; Parsons, S.; Parkin, A.; Boyd, G.; Jodrell, D. I.; Sadler, P. J. *J. Med. Chem.* **2001**, *44*, 3616−3621.

5.88 (d, 1H, $J = 5.5$ Hz), 4.41 (m, 2H), 2.71 (sep, 1H, $J = 6.9$ Hz), 2.17 (s, 3H), 1.25 (d, 3H, $J = 6.8$ Hz), 1.19 (d, 3H, $J = 6.6$ Hz).

**[($\eta^6$-*p*-cym)Os(bipy)Cl]$PF_6$ ($\mathbf{4PF_6}$).** A solution of 2,2′-bipyridine (21.1 mg, 0.14 mmol) and [($\eta^6$-*p*-cym)$OsCl_2$]$_2$ (51.1 mg, 0.07 mmol) in 4 mL methanol was stirred for 19 h at ambient temperature. It was then filtered through a glass wool plug, and a filtered solution of $NH_4PF_6$ (100 mg, ∼5 mol equiv) in 2 mL of MeOH was added. The solvent volume was reduced on a rotary evaporator to ∼3 mL. A yellow precipitate formed as the solution cooled to ambient temperature. The product was recovered by filtration, washed with methanol (4 mL) and diethyl ether (10 mL), and air-dried. Yield: 63.2 mg (74%). Anal. Calcd for $C_{20}ClH_{22}N_2OsPF_6$ (661.05): C, 36.34; H 3.35; N 4.24%. Found: C, 36.19; H, 3.36; N, 4.08%. $^1$H NMR ($CDCl_3$): $\delta$ 9.24 (d, 2H, $J = 5.6$ Hz), 8.26 (d, 2H, $J = 8.0$ Hz), 8.09 (dd, 2H, $J = 8.7$ and 7.8 Hz), 7.67 (dd, 2H, $J = 7.8$ and 6.6 Hz), 6.11 (d, 2H, $J = 5.8$ Hz), 5.86 (d, 2H, $J = 5.7$ Hz), 2.57 (sep, 1H, $J = 6.9$ Hz), 2.32 (s, 3H), 1.05 (d, 6H, $J = 6.9$ Hz).

**[($\eta^6$-*p*-cym)Os(phen)Cl]$PF_6$ ($\mathbf{5PF_6}$).** A solution of 1,10-phenanthroline (23.6 mg, 0.13 mmol) in 1 mL of methanol was added to a solution of [($\eta^6$-*p*-cym)$OsCl_2$]$_2$ (49.1 mg, 0.06 mmol) in 3 mL of methanol, and the mixture was stirred at 323 K for 1 h under argon. The solution was filtered through a glass wool plug, and the solvent volume was reduced to ∼2 mL on a rotary evaporator. A filtered solution of $NH_4PF_6$ (100 mg, ∼5 mol equiv) in 2 mL of MeOH was added, and the solvent was removed in vacuo. The residue was sonicated in ethanol to give a bright yellow suspension. The yellow powder was recovered by filtration, washed with ethanol (10 mL) and diethyl ether (10 mL), and air-dried. Yield: 67.4 mg (79%). Anal. Calcd for $C_{22}ClH_{22}N_2OsPF_6$ (685.04): C, 38.57; H 3.24; N 4.09%. Found: C, 38.61; H, 3.15; N, 3.96%. $^1$H NMR ($CDCl_3$): $\delta$ 9.59 (d, 2H, $J = 5.3$ Hz), 8.57 (d, 2H, $J = 8.2$ Hz), 8.07 (s, 2H), 8.03 (dd, 2H, $J = 8.2$ and 5.3 Hz), 6.27 (d, 2H, $J = 5.9$ Hz), 6.03 (d, 2H, $J = 5.8$ Hz), 2.57 (sep, 1H, $J = 6.9$ Hz), 2.29 (s, 3H), 1.00 (d, 6H, $J = 6.9$ Hz). Crystals suitable for X-ray diffraction were obtained by diffusion of hexane into a solution of $\mathbf{5PF_6}$ in chloroform at ambient temperature.

**[($\eta^6$-bip)Os(dppz)Cl]$PF_6$ ($\mathbf{6PF_6}$).** A solution of [($\eta^6$-bip)$OsCl_2$]$_2$ (22.3 mg, 0.03 mmol) was refluxed in MeOH (5 mL)/ $H_2O$ (2.5 mL) for 2 h under argon and then filtered through a cotton wool plug to remove a dark black precipitate. A solution of dppz (15.8 mg, 0.06 mmol) in 5 mL of MeOH was added to the resulting pale yellow filtrate. The reaction mixture was stirred at 323 K for 80 min under argon. The mixture was filtered through a glass wool plug, and the solvent volume was reduced on a rotary evaporator (to ∼5 mL). The addition of a filtered solution of $NH_4PF_6$ (90 mg, ∼10 mol equiv) in 1 mL of MeOH gave rise to a yellow precipitate which was recovered by filtration, washed with methanol (5 mL) and diethyl ether (10 mL), and air-dried. Yield: 32.5 mg (75%). Anal. Calcd for (**6** + $CH_3OH$) $C_{31}ClH_{24}N_4OOsPF_6$ (839.20): C, 44.37; H 2.88; N 6.68%. Found: C, 43.61; H, 2.43; N, 7.15%. $^1$H NMR (DMSO-$d_6$): $\delta$ 9.80 (d, 2H, $J = 5.6$ Hz), 9.73 (d, 2H, $J = 8.4$ Hz), 8.56 (dd, 2H, $J = 6.6$ and 3.5 Hz), 8.24 (dd, 2H, $J = 6.7$ and 3.4 Hz), 8.21 (dd, 2H, $J = 8.3$ and 5.6 Hz), 7.60 (d, 2H, $J = 7.9$ Hz), 7.56 (t, 1H, $J = 7.1$ Hz), 7.40 (t, 2H, $J = 7.7$ Hz), 7.02 (d, 2H, $J = 6.0$ Hz), 6.86 (t, 2H, $J = 5.8$ Hz), 6.49 (t, 1H, $J = 5.6$ Hz). Crystals suitable for X-ray diffraction were obtained by diffusion of diethyl ether into a solution of $\mathbf{6PF_6}$ in methanol at ambient temperature.

**[($\eta^6$-bip)Os(azpy-$NMe_2$)Cl]$PF_6$ ($\mathbf{7PF_6}$).** A solution of [($\eta^6$-bip)$OsCl_2$]$_2$ (50.7 mg, 0.06 mmol) in 10 mL of MeOH was refluxed for 3 h under argon and hot-filtered to remove a dark black precipitate. A solution of azpy-$NMe_2$ (4-(2-pyridylazo)-*N*,*N*-dimethylaniline) (35.3 mg, 0.16 mmol) in 5 mL of MeOH was added dropwise to the resulting pale yellow filtrate, which resulted in an instant color change to blue. The resulting mixture was stirred at ambient temperature for 1 h under argon. The solvent volume was reduced to ∼10 mL; $NH_4PF_6$ (114 mg, >10 mol equiv) added, and the mixture was left at 253 K overnight. The blue precipitate was recovered by filtration, washed with ethanol (20 mL) and diethyl ether (10 mL), and air-dried. The product was recrystallized from dichloromethane. Yield: 66.4 mg (73%). ESI-MS Calcd for $C_{25}ClH_{24}N_4Os$: *m*/*z* 607.1. Found: *m*/*z* 607.4. $^1$H NMR ($CDCl_3$): $\delta$ 8.57 (d, 1H, $J = 5.7$ Hz), 8.31 (d, 1H, $J = 7.6$ Hz), 8.00 (d, 2H, $J = 8.7$ Hz), 7.94 (t, 1H, $J = 7.9$ Hz), 7.50 (m, 5H), 7.32 (t, 1H, $J = 7.9$ Hz), 6.64 (d, 2H, $J = 8.7$ Hz), 6.50 (t, 2H, $J = 6.8$ Hz), 6.23 (t, 2H, $J = 5.7$ Hz), 6.15 (t, 1H, $J = 5.7$ Hz), 3.30 (s, 6H). Crystals suitable for X-ray diffraction were obtained by diffusion of diethyl ether into a solution of $\mathbf{7PF_6}$ in methanol at ambient temperature.

**[($\eta^6$-*p*-cym)Os(azpy-$NMe_2$)Cl]$PF_6$ ($\mathbf{8PF_6}$).** The dropwise addition of a solution of azpy-$NMe_2$ (31.6 mg, 0.14 mmol) in 4 mL of MeOH to a solution of [($\eta^6$-*p*-cym)$OsCl_2$]$_2$ (55.5 mg, 0.07 mmol) in 15 mL of MeOH, resulted in an instant color change to blue. The resulting mixture was stirred at ambient temperature for 6.5 h under argon, and the solvent volume was then reduced to ∼5 mL on a rotary evaporator. Blue crystals formed overnight at 253 K after the addition of $NH_4PF_6$ (100 mg, ∼5 mol equiv) to the solution. The product was recovered by filtration, washed with ethanol (20 mL) and diethyl ether (10 mL), air-dried, and recrystalized from dichloromethane. Yield: 92.1 mg (90%). Anal. Calcd for $C_{23}ClH_{28}N_4OsPF_6$ (731.12): C, 37.78; H 3.86; N 7.66%. Found: C, 37.81; H, 3.74; N, 7.67%. $^1$H NMR ($CDCl_3$): $\delta$ 9.18 (d, 1H, $J = 5.8$ Hz), 8.32 (d, 1H, $J = 7.9$ Hz), 8.06 (d, 2H, $J = 9.0$ Hz), 8.00 (t, 1H, $J = 7.7$ Hz), 7.62 (t, 1H, $J = 6.6$ Hz), 6.77 (d, 2H, $J = 9.2$ Hz), 6. 25 (d, 1H, $J = 5.7$ Hz), 6.03 (d, 1H, $J = 5.8$ Hz), 5.93 (d, 1H, $J = 5.8$ Hz), 5.82 (d, 1H, $J = 5.6$ Hz), 3.32 (s, 6H), 2.34 (s, 3H), 2.33 (sept, 1H, $J = 7.0$ Hz), 0.96 (d, 3H, $J = 7.0$ Hz), 0.87 (d, 3H, $J = 6.9$ Hz). Crystals suitable for X-ray diffraction were obtained by slow evaporation of a methanol solution of $\mathbf{8PF_6}$ at ambient temperature.

**[($\eta^6$-bip)Os($NCCH_3$-*N*)$Cl_2$] (9).** Acetonitrile (0.5 mL) was added to a suspension of [($\eta^6$-bip)$OsCl_2$]$_2$ (98 mg, 0.12 mmol) in dichloromethane (6 mL), and the reaction mixture was heated (320 K) with stirring under argon, shielded from light, for 3 h. The reaction mixture was filtered; the volume of the filtrate was reduced (to 4 mL) on a rotary evaporator, and diethyl ether was added until yellow crystals began to form. After the mixture stood at 253 K overnight, the yellow crystals were recovered by filtration, washed with diethyl ether (5 mL) and hexane (5 mL), and air-dried. Yield: 80.7 mg (76%). Anal. Calcd for $C_{14}Cl_2H_{13}NOs$ (456.40): C, 36.84; H 2.87; N 3.07%. Found: C, 36.24; H, 2.69; N, 2.80%. $^1$H NMR (DMSO-$d_6$): $\delta$ 7.70 (d, 2H, $J = 7.9$ Hz), 7.45 (m, 3H), 6.66 (d, 2H, $J = 5.5$ Hz), 6.36 (t, 1H, $J = 5.1$ Hz), 6.32 (t, 2H, $J = 5.1$ Hz), 2.07 (s, 3H). Crystals of **9** suitable for X-ray diffraction were obtained by diffusion of diethyl ether into an aliquot of the original reaction mixture, at ambient temperature in the dark.

**Instrumentation. X-ray Crystallography.** All diffraction data were collected using a Bruker (Siemens) Smart Apex CCD diffractometer equipped with an Oxford Cryosystems low-temperature device operating at 150 K. Absorption corrections for all data sets were performed with the multiscan procedure SADABS;[25]

(25) Sheldrick, G. M. *SADABS*; University of Göttingen: Germany, 2001−2004.

structures were solved using direct methods (SHELXL,[26] SIR92,[27] or DIRDIF[28]). The complexes were refined against $F^2$ using SHELXTL, and the H-atoms were placed in geometrically calculated positions. X-ray crystallographic data for complexes **1PF$_6$**, **2BF$_4$**, and **5PF$_6$**−**9** are available as Supporting Information and have been deposited in the Cambridge Crystallographic Data Centre under the accession numbers CCDC 630298, 630299, 630300, 630301, 630303, 630302, and 630304, respectively.

**NMR Spectroscopy.** $^1$H NMR spectra were acquired on a Bruker AVA 600 ($^1$H = 600 MHz) spectrometer. $^1$H NMR spectra in $D_2O$ were typically acquired with water suppression by Shaka[29] or presaturation methods. $^1$H NMR chemical shifts were internally referenced to 1,4-dioxane (3.75 ppm) for aqueous solutions, (C*H*D$_2$)(CD$_3$)SO (2.50 ppm) for DMSO-$d_6$, CD$_2$*H*OD (3.34 ppm) for methanol-$d_4$, and C*H*Cl$_3$ (7.26 ppm) for chloroform-$d_1$ solutions. All data processing was carried out using XWIN-NMR, version 3.6 (Bruker U.K. Ltd.).

**Mass Spectrometry.** Electrospray ionization mass spectra (ESI-MS) were obtained on a Micromass Platform II Mass Spectrometer and $D_2O/H_2O$ solutions were infused directly. The capillary voltage was 3.5 V, and the cone voltage was varied between 20 and 45 V depending on sensitivity. The source temperature was 353 K. Mass spectra were recorded with a scan range of $m/z$ 200−1000 for positive ions.

**pH* Measurement.** The pH* (pH meter reading without correction for effects of D on glass electrode) values of NMR samples in $D_2O$ were measured at ∼298 K directly in the NMR tube, before and after the NMR spectra were recorded, using a Corning 240 pH meter equipped with a microcombination electrode calibrated with Aldrich buffer solutions at pH 4, 7, and 10.

**Methods. Kinetics of Hydrolysis.** The kinetics of the hydrolysis of complexes **1BF$_4$**−**5PF$_6$** were monitored at various temperatures by preparation of 0.8 mM solutions, prepared in methanol-$d_4$ (5% final), followed by subsequent dilution (1:20 v/v) with $D_2O$ (pH* ≈ 2, so that deprotonation of the aqua ligand is prevented) at the required temperature. Samples were filtered and placed in the NMR spectrometer preset at the desired temperature, and spectra were recorded at various time intervals. Data, based on peak integrals, were fitted to first-order kinetics to give the rate constant (k). The Arrhenius activation energies ($E_a$), activation enthalpies ($\Delta H^{\ddagger}$), and activation entropies ($\Delta S^{\ddagger}$) were determined from the slopes of the Arrhenius and (intercepts of) Eyring plots. The kinetics of hydrolysis and p$K_a^*$ values of coordinated water of complexes **6PF$_6$**, **7PF$_6$**, and **8PF$_6$** were not determined because of the poor aqueous solubility of these complexes.

To study the aqueous stability of complex **9**, a 2 mM solution was prepared in $D_2O$, and its $^1$H NMR spectrum was recorded directly after sample preparation (∼15 min).

**Determination of p$K_a^*$ Values.** For determination of p$K_a^*$ values (p$K_a$ values for $D_2O$ solutions), the pH* values of solutions of the aqua complexes **2A**−**5A** in $D_2O$ (formed in situ by hydrolysis of the parent chloro complexes **2BF$_4$**−**5PF$_6$**) were varied from pH* ∼2 to 10 by the addition of dilute NaOD and $HNO_3$, and the $^1$H NMR spectra were recorded. The chemical shifts of the arene ring protons were plotted against pH*. The pH* titration curves were fitted to the Henderson−Hasselbalch equation, with the assumption that the observed chemical shifts are weighted averages according to the populations of the protonated and deprotonated species. These p$K_a^*$ values can be converted to p$K_a$ values by use of the equation p$K_a$ = 0.929p$K_a^*$ + 0.42 as suggested by Krezel and Bal,[30] for comparison with related values in the literature.

**Interactions with Nucleobases.** The reaction of complex **3PF$_6$** with 9-ethylguanine (9EtG) at pH* 7.4 and 310 K was monitored over time using $^1$H NMR spectroscopy by mixing equal amounts of equilibrium $D_2O$ solutions (1 mM) of **3PF$_6$** and 9EtG. The pH* values of these solutions were adjusted with dilute NaOH to remain close to physiological pH* 7.4, and the solutions were allowed to equilibrate at 310 K before mixing. Their $^1$H NMR spectra were recorded at 310 K after various time intervals.

Similarly, equal volumes of equilibrium solutions of **1BF$_4$** and 5′-GMP in $D_2O$ were mixed at 298 K (final concentration 1.6 mM, pH* 6.9), and $^1$H NMR spectra recorded at various time intervals. To determine the Os$^{II}$ binding sites on 5′-GMP, a pH* titration over the range 2−12 was monitored by $^1$H NMR spectroscopy, and the chemical shifts of the H8 signals were plotted against pH*.

Solutions containing **1BF$_4$** or the ruthenium analogue, [($\eta^6$-bip)-Ru(en)Cl]PF$_6$ (**1R**), and 1 mol equiv 9EtG were prepared in $D_2O$ at various concentrations (1 mM, 500, 250, 100, and 50 $\mu$M), and after incubation at 310 K for 24 h (to reach equilibrium), their $^1$H NMR spectra were recorded at 298 K. Binding constants (log $K$) for 9EtG were obtained from the slopes of plots of [bound 9EtG]/[free 9EtG] versus [free metal complex], based on peak integrals.

In addition, a 1:1 stock solution of **1BF$_4$** and 9EtG (1 mM), which had already been allowed to reach equilibrium (24 h at 310 K), was diluted to give solutions of 500, 250, 100, and 50 $\mu$M. These were incubated at 310 K for a further 24 h before their $^1$H NMR spectra were recorded at 298 K.

**Cytotoxicity Toward A2780 and A549 Human Cancer Cells.** After they were plated, human ovarian A2780 cancer cells were treated with Os$^{II}$ complexes on day 3, and human lung A549 cancer cells were treated on day 2, at concentrations ranging from 0.1 to 100 $\mu$M. Solutions of the Os$^{II}$ complexes were made up in 0.125% DMSO to assist dissolution. Cells were exposed to the complexes for 24 h, washed, supplied with fresh medium, and allowed to grow for three doubling times (72 h), and then the protein content measured (proportional to cell survival) using the sulforhodamine B (SRB) assay.[31]

**Stability Studies.** The stabilities of complexes **1PF$_6$**, **1BF$_4$**, and **2BF$_4$** were investigated by preparation of 1 mM solutions in 5% MeOD-$d_4$/95% isotonic saline solution (150 mM NaCl) by dissolution of the complex in MeOD-$d_4$, followed by rapid dilution with the isotonic saline solution. $^1$H NMR spectra were recorded after various time intervals (10 min, 1 week, 2 weeks, and 2 months) during which time the sample was stored at ambient temperature in the dark.

The stability of **1BF$_4$** in DMSO under various conditions was also investigated. Two solutions (∼4 mM) of **1BF$_4$** were prepared in DMSO-$d_6$, and their $^1$H NMR spectra were recorded directly after sample preparation (<10 min). One sample was stored at ambient temperature, stoppered in the dark for 24 h, and one was exposed to heat, sonication, sunlight, and air for 24 h, before its $^1$H NMR spectrum was recorded.

(26) Sheldrick, G. M.. *SHELXL-97, Program for the refinement of crystal structures*; University of Göttingen: Göttingen, Germany, 1997.
(27) Altomare, A.; Cascarano, G.; Giacovazzo, G.; Guagliardi, A.; Burla, M. C.; Polidori, G.; Camalli, M. *J. Appl. Crystallogr.* **1994**, *27*, 435−435.
(28) Beurskens, P. T.; Beurskens, G.; Bosman, W. P.; de Gelder, R.; Garcia-Granda, S.; Gould, R. O.; Israel, R.; Smits, J. M. M. *DIRDIF*; Crystallography Laboratory, University of Nijmegen: Nijmegen, The Netherlands, 1996.
(29) Hwang, T. L.; Shaka, A. J. *J. Magn. Reson., Ser. A* **1995**, *112*, 275−279.
(30) Krezel, A.; Bal, W. *J. Inorg. Biochem.* **2004**, *98*, 161−166.
(31) Skehan, P.; Storeng, R.; Scudiero, D.; Monks, A.; McMahon, J.; Vistica, D.; Warren, J. T.; Bokesch, H.; Kenney, S.; Boyd, M. R. *J. Natl. Cancer Inst.* **1990**, *82*, 1107−1112.

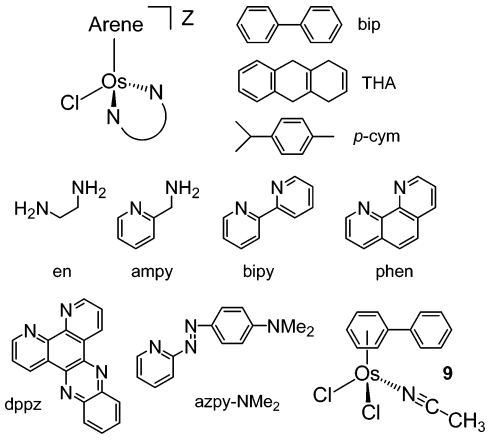


| Compound | Arene | N-N | Z |
|---|---|---|---|
| **1PF$_6$/BF$_4$** | bip | en | $PF_6/BF_4$ |
| **2BF$_4$** | THA | en | $BF_4$ |
| **3PF$_6$** | *p*-cym | ampy | $PF_6$ |
| **4PF$_6$** | *p*-cym | bipy | $PF_6$ |
| **5PF$_6$** | *p*-cym | phen | $PF_6$ |
| **6PF$_6$** | bip | dppz | $PF_6$ |
| **7PF$_6$** | bip | azpy-$NMe_2$ | $PF_6$ |
| **8PF$_6$** | *p*-cym | azpy-$NMe_2$ | $PF_6$ |
| **9** | bip | $NCCH_3$ Cl | - |

**Figure 1.** Osmium(II) arene complexes containing N-donor ligands studied in this work.

## Results

Monofunctional (chlorido) osmium(II) arene complexes containing neutral diamine or azopyridine N,N-chelating ligands, as well as the bifunctional complex [($\eta^6$-bip)Os(NCCH$_3$-*N*)Cl$_2$] (**9**), Figure 1, were synthesized in good yields via the Cl-bridged dimers, [($\eta^6$-arene)OsCl$_2$]$_2$ where arene = biphenyl (bip), tetrahydroanthracene (THA), or *p*-cymene (*p*-cym). They were characterized by elemental analysis or ESI-MS, NMR spectroscopy, and for seven complexes, X-ray crystallography.

**X-ray Crystal Structures.** The X-ray crystal structures of [($\eta^6$-bip)Os(en)Cl]PF$_6$ (**1PF$_6$**), [($\eta^6$-THA)Os(en)Cl]BF$_4$ (**2BF$_4$**), [($\eta^6$-*p*-cym)Os(phen)Cl]PF$_6$ (**5PF$_6$**), [($\eta^6$-*p*-cym)Os(dppz)Cl]PF$_6$ (**6PF$_6$**), [($\eta^6$-bip)Os(azpy-NMe$_2$)Cl]PF$_6$ (**7PF$_6$**), [($\eta^6$-*p*-cym)Os(azpy-NMe$_2$)Cl]PF$_6$ (**8PF$_6$**), and [($\eta^6$-bip)Os(NCCH$_3$-*N*)Cl$_2$] (**9**) were determined. Their structures and atom numbering schemes are shown in Figure 2. The complexes adopt the expected pseudo-octahedral "three-leg piano-stool" geometry with the osmium $\pi$-bonded to the arene ligand (1.65−1.71 Å to centroid of ring), $\sigma$-bonded to a chloride (2.41−2.37 Å) and the two nitrogen atoms of the chelate (2.02−2.15 Å), which constitute the three legs of the piano stool. Crystallographic data and selected bond lengths and angles are shown in Tables 1 and 2.

Complex **1PF$_6$** crystallizes with 2 independent molecules in the unit cell. The biphenyl unit is twisted (by 27 or 43°), and intermolecular arene ring stacking is observed between the coordinated arene in two independent molecules (4.34 Å at a dihedral angle of 32.4°). In contrast, the coordinated THA ligand in complex **2BF$_4$** is almost planar, being slightly bent upward (away from the legs) by 6.5°. Adjacent

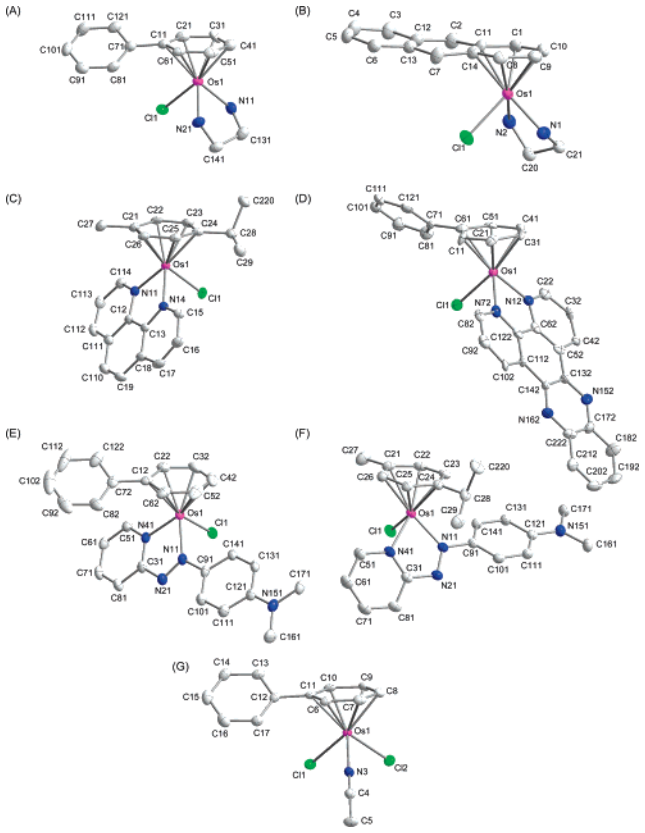


**Figure 2.** X-ray structures and atom numbering schemes for complexes (A) [($\eta^6$-bip)Os(en)Cl]PF$_6$ **1PF$_6$**, (B) [($\eta^6$-THA)Os(en)Cl]BF$_4$ **2BF$_4$**, (C) [($\eta^6$-*p*-cym)Os(phen)Cl]PF$_6$ **5PF$_6$**, (D) [($\eta^6$-bip)Os(dppz)Cl]PF$_6$ **6PF$_6$**, (E) [($\eta^6$-bip)Os(azpy-NMe$_2$)Cl]PF$_6$ **7PF$_6$**, (F) [($\eta^6$-*p*-cym)Os(azpy-NMe$_2$)Cl]PF$_6$ **8PF$_6$**, and (G) [($\eta^6$-bip)Os(NCCH$_3$-*N*)Cl$_2$] **9** (50% probability ellipsoids). The H atoms and counterions have been omitted for clarity.

molecules crystallize with their arenes parallel, see Figure S1. The distance between the THA ligands is 3.3 Å, and the rings are separated by 4.13, 4.10, and 4.13 Å at dihedral angles of 32, 27, and 32°, respectively. Further intermolecular arene ring stacking is observed in the crystal structures of complex **5PF$_6$** and the twinned complex **6PF$_6$**, between one of the bound pyridine rings and the related pyridine of a second molecule (3.72 and 4.75 Å at dihedral angles of 37.0 and 40.0°, respectively), Figure S2. The biphenyl ligands in the crystal structures of **6PF$_6$** and **7PF$_6$** are twisted by 33 and 32°, respectively. Arene ring stacking was also observed in the crystal structure of **7PF$_6$**, between the coordinated pyridine and the phenyl ring attached to the azo group of an adjacent molecule (4.7 Å at a dihedral angle of 50°), but not in that of complex **8PF$_6$**. Complex **9**, in which the biphenyl is twisted by 42°, crystallizes such that dimers link four independent molecules through chloride ligand (Cl1) of one molecule and the arene protons C8H81 and C5H51 of two others (C8···Cl1 = 3.513(5) Å and C5···Cl1 3.680(6) Å, respectively), Figure S3. The $PF_6^-$ and $BF_4^-$ counterions in these crystal structures are extensively involved in H-bonding to the chelated ligand or arene protons.

**Kinetics of Hydrolysis.** The rate of hydrolysis of complex **3PF$_6$** at 298 K in aqueous solution ($D_2O$) was monitored at pH* values of 8, 6 and 2. The rate of hydrolysis, based on peak integrals for *p*-cymene peaks, of the intact chloro complex **3** (5.93 and 5.91 ppm) and the aqua complex **3A**

**Table 1.** Crystallographic Data for [($\eta^6$-bip)Os(en)Cl]$PF_6$, **1PF$_6$**, [($\eta^6$-THA)Os(en)Cl]$BF_4$, **2BF$_4$**, [($\eta^6$-*p*-cym)Os(phen)Cl]$PF_6$, **5PF$_6$**, [($\eta^6$-*p*-cym)Os(dppz)Cl]$PF_6$, **6PF$_6$**, [($\eta^6$-bip)Os(azpy-$NMe_2$)Cl]$PF_6$, **7PF$_6$**, [($\eta^6$-*p*-cym)Os(azpy-$NMe_2$)Cl]$PF_6$, **8PF$_6$**, and [($\eta^6$-bip)Os($NCCH_3$-*N*)$Cl_2$], **9**

| | **1PF$_6$** | **2BF$_4$** | **5PF$_6$** | **6PF$_6$** | **7PF$_6$** | **8PF$_6$** | **9** |
|---|---|---|---|---|---|---|---|
| formula | $C_{14}H_{18}ClF_6N_2OsP$ | $C_{16}H_{22}BClF_4N_2Os$ | $C_{22}H_{22}ClF_6N_2OsP$ | $C_{30}H_{21}ClF_6N_4OsP$ | $C_{50}H_{48}Cl_2F_{12}N_8Os_2P_2$ | $C_{46}H_{56}Cl_2F_{12}N_8Os_2P_2$ | $C_{14}H_{13}Cl_2NOs$ |
| MW | 584.92 | 554.82 | 685.04 | 807.13 | 751.11 | 731.12 | 456.37 |
| cryst description | colorless block | yellow plate | yellow block | yellow lath | dark green prism | black block | yellow plate |
| cryst size (mm) | 0.08 × 0.08 × 0.34 | 0.09 × 0.15 × 0.44 | 0.14 × 0.16 × 0.36 | 0.13 × 0.16 × 0.61 | 0.17 × 0.22 × 0.26 | 0.33 × 0.52 × 0.55 | 0.17 × 0.42 × 0.81 |
| $\lambda$ (Å) | 0.71073 | 0.71073 | 0.71073 | 0.71073 | 0.71073 | 0.71073 | 0.71073 |
| temp (K) | 150 | 150 | 150 | 150 | 150 | 150 | 150 |
| cryst syst | monoclinic | monoclinic | orthorhombic | monoclinic, twinned | triclinic | triclinic | monoclinic |
| space group | *P*121/*c*1 | *P*121/*n*1 | P*bca* | *P*121/*c*1 | $P\bar{1}$ | $P\bar{1}$ | *P*121/*c*1 |
| *a* (Å) | 19.5853(8) | 12.722(3) | 12.7769(3) | 11.8153(12) | 8.1226(3) | 8.2549(3) | 10.0020(15) |
| *b* (Å) | 9.0300(4) | 7.9298(16) | 13.3958(2) | 8.7125(9) | 10.0165(4) | 12.2787(4) | 7.009(1) |
| *c* (Å) | 23.2542(8) | 18.142(4) | 26.6395(6) | 26.175(3) | 17.3516(6) | 12.8556(5) | 19.717(3) |
| α (deg) | 90 | 90 | 90 | 90 | 101.105(2) | 84.792(2) | 90 |
| $\beta$ (deg) | 112.608(2) | 105.28(3) | 90 | 102.952(4) | 96.365(2) | 82.980(2) | 102.447(2) |
| $\gamma$ (deg) | 90 | 90 | 90 | 90 | 109.271(2) | 80.680(2) | 90 |
| vol (Å$^3$) | 3796.6(3) | 1765.6(7) | 4559.53(16) | 2626.0(5) | 1284.28(9) | 1272.84(8) | 1349.8(3) |
| *Z* | 8 | 4 | 8 | 4 | 1 | 1 | 4 |
| $R(F_o^2)$ | 0.0913 | 0.0307 | 0.048 | 0.043 | 0.039 | 0.031 | 0.0285 |
| $R_w(F_o^2)$ | 0.0972 | 0.0907 | 0.066 | 0.045 | 0.077 | 0.065 | 0.0802 |
| GOF | 0.6814 | 0.9498 | 0.599 | 1.056 | 0.941 | 0.665 | 1.0434 |

**Table 2.** Selected Bond Lengths (Å) and Angles (deg) for [($\eta^6$-bip)Os(en)Cl]$PF_6$, **1PF$_6$**, [($\eta^6$-THA)Os(en)Cl]$BF_4$, **2BF$_4$**, [($\eta^6$-*p*-cym)Os(phen)Cl]$PF_6$, **5PF$_6$**, [($\eta^6$-*p*-cym)Os(dppz)Cl]$PF_6$, **6PF$_6$**, [($\eta^6$-bip)Os(azpy-$NMe_2$)Cl]$PF_6$, **7PF$_6$**, [($\eta^6$-*p*-cym)Os(azpy-$NMe_2$)Cl]$PF_6$, **8PF$_6$**, and [($\eta^6$-bip)Os($NCCH_3$-*N*)$Cl_2$], **9**[a]

| | **1PF$_6$** | **2BF$_4$** | **5PF$_6$** | **6PF$_6$** | **7PF$_6$** | **8PF$_6$** | **9** |
|---|---|---|---|---|---|---|---|
| Os−C(arene) | 2.232(7) | 2.156(5) | 2.196(3) | 2.215(8) | 2.220(4) | 2.278(4) | 2.178(4) |
| | 2.208(7) | 2.180(5) | 2.208(3) | 2.192(7) | 2.207(5) | 2.209(4) | 2.193(5) |
| | 2.195(7) | 2.224(4) | 2.187(3) | 2.195(5) | 2.189(5) | 2.214(3) | 2.181(4) |
| | 2.176(8) | 2.171(5) | 2.224(3) | 2.139(7) | 2.219(5) | 2.220(3) | 2.170(4) |
| | 2.169(7) | 2.218(5) | 2.194(4) | 2.173(8) | 2.211(5) | 2.175(3) | 2.183(5) |
| | 2.194(7) | 2.200(5) | 2.178(3) | 2.257(5) | 2.201(5) | 2.231(4) | 2.186(4) |
| Os−$N_1$ | 2.136(6) | 2.127(4) | 2.091(3) | 2.117(5) | 2.055(3) | 2.055(3) | 2.057(4) |
| Os−$X_2$ | 2.152(6) | 2.140(4) | 2.094(3) | 2.073(5) | 2.071(4) | 2.021(3) | 2.4139(12) |
| Os−Cl | 2.3918(19) | 2.4107(12) | 2.4062(9) | 2.3958(14) | 2.3962(11) | 2.3711(8) | 2.3976(11) |
| $N_1$−Os−$X_2$ | 78.7(2) | 78.48(16) | 77.22(11) | 76.98(17) | 74.89(14) | 74.99(12) | 85.01(11) |
| $N_1$−Os−Cl | 83.47(17) | 82.88(12) | 83.17(8) | 85.14(17) | 85.10(10) | 83.26(8) | 84.00(11) |
| Cl−Os−$X_2$ | 83.65(18) | 81.87(11) | 83.06(8) | 84.69(17) | 83.94(10) | 87.17(8) | 86.14(4) |

[a] $X_2$ = second nitrogen donor group and $N_1$ = pyridine (and $X_2$ = azo) in **7PF$_6$** and **8PF$_6$**. For complex **9**, $X_2 = Cl_2$.

(5.76 and 5.74 ppm) was rapid at pH* 8, with a half-life of ~0.11 h. At pH* ~6, the rate of hydrolysis was slower ($t_{1/2}$ = 0.66 h), with less hydrolysis of the complex and at pH* ~2, even slower. A fit to pseudo-first-order kinetics yielded a rate constant of $k = 0.13\ h^{-1}$ ($t_{1/2}$ = 5.3 h, Figure 3A) at pH* 2.

A comparison of the rates of hydrolysis of complexes **1BF$_4$**, **2BF$_4$**, **3PF$_6$**, **4PF$_6$**, and **5PF$_6$** under acidic aqueous conditions ($D_2O$, pH* ~2), to prevent deprotonation of the coordinated water (Figure 3B and Table 3), showed that the rates decrease in the order **3PF$_6$** > **2BF$_4$** > **1BF$_4$** ≫ **4PF$_6$** ≈ **5PF$_6$**. From the data obtained at various temperatures, the Arrhenius activation energies ($E_a$), activation enthalpies ($\Delta H^{\ddagger}$), and activation entropies ($\Delta S^{\ddagger}$) were determined, Figure S4 and Table 3. The large negative $\Delta S^{\ddagger}$ values for complexes **1BF$_4$**, **2BF$_4$**, and **3PF$_6$** are notable.

The $^1$H NMR spectrum of a solution of complex **9**, [($\eta^6$-bip)Os($NCCH_3$)$Cl_2$], in $D_2O$ (2 mM) showed peaks for a number of minor unidentified species and major arene peaks (~60% of species) at 6.46, 6.25, and 6.01 ppm assignable to the trihydroxo-bridged dimer, [($\eta^6$-bip)Os($\mu$-OD)$_3$Os($\eta^6$-bip)]$^+$, Figure 4.[19]

**p$K_a^*$ Determination.** Peaks for coordinated arene-ring protons of the aqua complexes, [($\eta^6$-arene)Os(NN)($OD_2$)]$^{2+}$ **2A**−**5A**, shifted to high field with increase in pH*. The chemical shifts were plotted against pH* (Figure S5), and the data were fitted to the Henderson−Hasselbalch equation, from which the p$K_a^*$ values of the coordinated water were determined. This yielded a value of 5.8 for complexes containing two $\pi$-acceptor pyridine groups as N-donors (**4A**/**5A**) and 6.3 for complexes containing a primary amine as N-donor (**2A**/**3A**), see Table 4.

**Guanine Adducts.** New peaks, assignable to the adduct [($\eta^6$-*p*-cym)Os(ampy)(9EtG)]$^{2+}$ **3G**, appeared in the $^1$H NMR spectrum of **3PF$_6$** and 9EtG (1:1, 0.5 mM) over time and under biologically relevant conditions (pH* ~7.4, 310 K), Figure 5A. On the basis of peak integration, the reaction half-life was ~3.2 h (Figure 5B).

Similarly, new peaks appeared over time in the H8 region in $^1$H NMR spectra of 1:1 solutions of **1BF$_4$** and 5′-GMP (1.6 mM, $D_2O$, pH* 6.9, 298 K). After 30 h, ~40% of the 5′-GMP had reacted, Figure 6A. The H8 peak for free 5′-GMP (8.15 ppm, **b**), decreased in intensity with an approximate half-life of ~8.5 h, and peaks for new species **a**

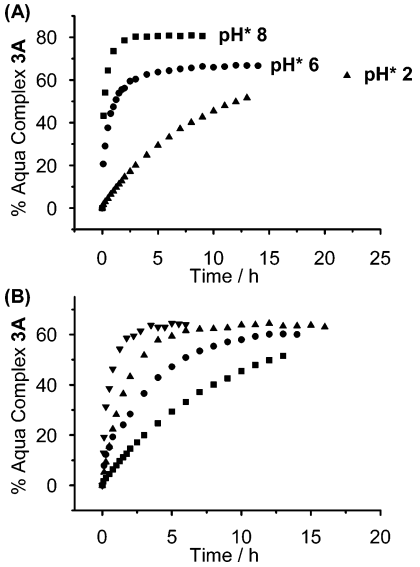


**Figure 3.** Time dependence for formation of the aqua complex **3A** (based on $^1$H NMR peak integrals) during hydrolysis of $\mathbf{3PF_6}$ [($\eta^6$-*p*-cym)Os(ampy)Cl]$PF_6$ (A) at 298 K in $D_2O$ at various pH* values, 8 (■), 6 (●), and 2 (▲), giving half-lifes of ∼0.11, 0.66 and 5.3 h, respectively. (B) Hydrolysis of $\mathbf{3PF_6}$ in acidic $D_2O$ (pH* ∼2) at 298 K (■), 304 K (●), 310 K (▲), and 316 K (▼).

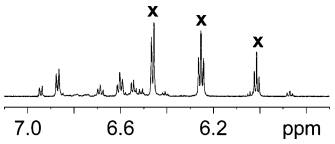


**Figure 4.** Formation of hydroxo-bridged dimer [($\eta^6$-bip)Os($\mu$-OD)$_3$Os($\eta^6$-bip)]$^+$ from [($\eta^6$-bip)Os(NCCH$_3$-*N*)Cl$_2$] **9** in aqueous solution. Low-field region of the $^1$H NMR spectrum, showing the coordinated biphenyl arene ring protons, of **9** in $D_2O$ within 15 min of sample preparation. Assignments: **x** corresponds to the hydroxo-bridged dimer, which accounts for ∼60% of {($\eta^6$-bip)Os}$^{2+}$ species present in solution. Other peaks have not been assigned.

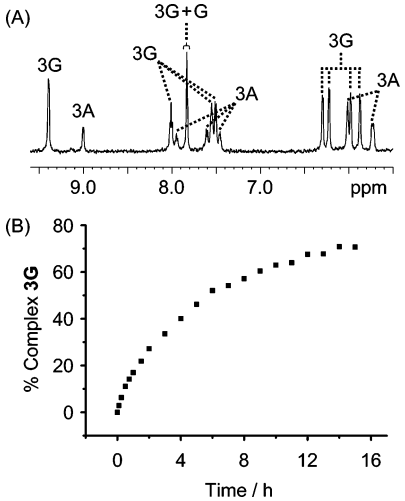


**Figure 5.** (A) Low-field region of the $^1$H NMR spectrum of an aqueous solution of $\mathbf{3PF_6}$ (0.5 mM) after reactiion with 1 mol equiv 9EtG for 15 h (pH* ≈ 7.4 and 310 K). Peak assignments: [($\eta^6$-*p*-cym)Os(ampy)(OD)]$^+$ **3A**, H8 of free 9EtG **G** and the 9EtG bound product [($\eta^6$-*p*-cym)Os(ampy)(9EtG)]$^{2+}$ **3G**. (B) Time dependence, based on $^1$H NMR peak integrals, for formation of [($\eta^6$-*p*-cym)Os(ampy)(9EtG)]$^{2+}$ (**3G**) in the above reaction.

(8.45 ppm) and **c** (8.03 ppm) appeared with half-lives of ∼8.5 and 9.0 h, respectively, with **c** forming before **a** (Figure 6B). Peaks were assigned and binding sites on 5′-GMP were

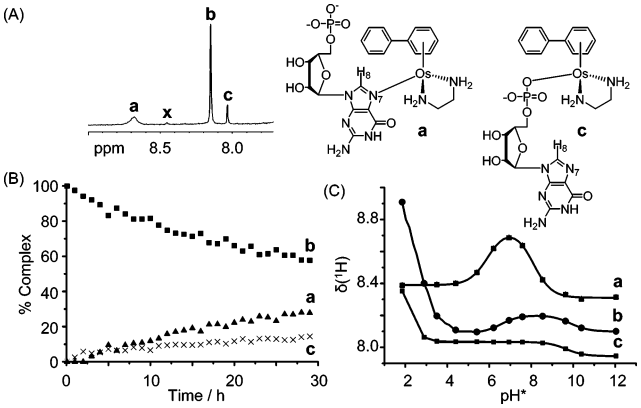


**Figure 6.** (A) Low-field region of the $^1$H NMR spectrum of an aqueous solution of $\mathbf{1BF_4}$ (1.6 mM) containing 1 mol equiv 5′-GMP after 30 h at 298 K. (B) Time dependence, based on $^1$H NMR peak integrals, of decay/formation of peaks **a**, **b**, and **c** from the above reaction. (C) pH* titrations of the reaction mixture. Plots of H8 chemical shift vs pH*. Solid curves are computer fits giving p$K_a^*$ values for **a** (5.94 and 8.09), **b** (2.55, 6.57, and 9.86), and **c** (0.95 and 9.66). Peak assignments (see structures): **a**, Os-*N7*GMP; **b**, free 5′-GMP; **c**, Os-*O*(PO$_3$)GMP; **x**, possible dinuclear complex Os-*O*(PO$_3$)GMP*N7*-Os.

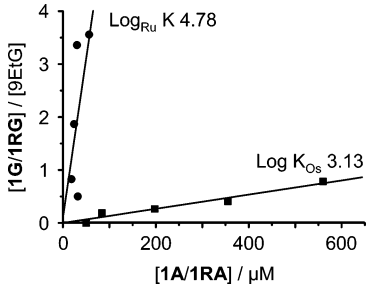


**Figure 7.** Determination of the apparent formation constants for the osmium and ruthenium analogues, [($\eta^6$-bip)Os(en)(9EtG)]$^{2+}$ (**1G**) and [($\eta^6$-bip)Ru(en)(9EtG)]$^{2+}$ (**1RG**). The extent of binding was determined by the integration of $^1$H NMR peaks (see Figure S5). From the slopes of the plots of [($\eta^6$-bip)M(en)(9EtG)]$^{2+}$/[free 9EtG] vs [($\eta^6$-bip)M(en)(OD$_2$)]$^{2+}$, the binding constants log $K = 3.13 \pm 0.03$ and $4.78 \pm 0.09$ were determined for Os$^{II}$ (**1G**) and Ru$^{II}$ (**1RG**), respectively.

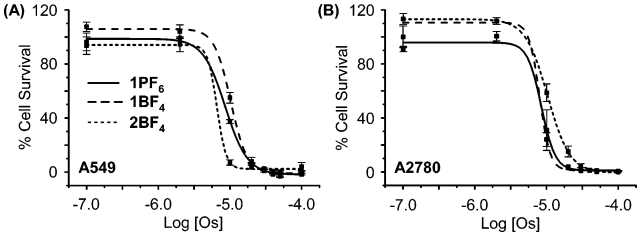


**Figure 8.** Cytotoxicity of [($\eta^6$-bip)Os(en)Cl]$PF_6$ (**1PF$_6$**, —), [($\eta^6$-bip)Os(en)Cl]$BF_4$ (**1BF$_4$**, — —), and [($\eta^6$-THA)Os(en)Cl]$BF_4$ (**2BF$_4$**, - - -) toward (A) human A549 lung cancer cells and (B) human A2780 ovarian cancer cells. The $IC_{50}$ values (concentrations that inhibit cell growth by 50%) obtained from these curves are given in Table 5.

established by monitoring a pH* titration of the mixture by $^1$H NMR spectroscopy (Figure 6C). Peak **b** for free 5′-GMP was assigned by addition of excess 5′-GMP to the mixture and shifted with pH* to give three p$K_a^*$ values of 2.55, 6.57, and 9.86, corresponding to N7H, the phosphate backbone, and N1H deprotonation, respectively. Peak **a** shifted with two associated p$K_a^*$ values of 5.94 and 8.09 (phosphate and N1H deprotonation), consistent with N7-bound 5′-GMP, [($\eta^6$-bip)Os(en)(5′-GMP-*N7*)]. Peak **c** shifted with two associated p$K_a^*$ values of 0.95 and 9.66 assignable to N7H and N1H

**Table 3.** Rate Data for the Aquation of Complexes **1BF$_4$**−**5PF$_6$** at Various Temperatures

| | $T$ (K) | $k$ ($h^{-1}$) | $t_{1/2}$ (h) | $E_a$ (kJ $mol^{-1}$) | $\Delta H^{\ddagger}$ (kJ $mol^{-1}$) | $\Delta S^{\ddagger}$ (J $K^{-1}$ $mol^{-1}$) |
|---|---|---|---|---|---|---|
| **1BF$_4$** | 298 | 0.046 ± 0.007 | 15.11 ± 0.22 | 101.2 ± 2.0 | 98.6 ± 2.0 | −60.6 ± 6.3 |
| | 310 | 0.250 ± 0.001 | 2.80 ± 0.08 | | | |
| | 318 | 0.615 ± 0.014 | 1.13 ± 0.03 | | | |
| | 333 | 3.439 ± 0.151 | 0.20 ± 0.01 | | | |
| **2BF$_4$** | 298 | 0.082 ± 0.001 | 8.47 ± 0.13 | 97.8 ± 4.1 | 95.1 ± 4.2 | −54.2 ± 13.3 |
| | 310 | 0.423 ± 0.009 | 1.64 ± 0.03 | | | |
| | 318 | 1.205 ± 0.052 | 0.58 ± 0.03 | | | |
| | 333 | 5.105 ± 0.232 | 0.14 ± 0.01 | | | |
| **3PF$_6$** | 298 | 0.131 ± 0.002 | 5.29 ± 0.08 | 94.3 ± 4.6 | 91.7 ± 4.6 | −46.2 ± 15.2 |
| | 304 | 0.308 ± 0.007 | 2.25 ± 0.05 | | | |
| | 310 | 0.545 ± 0.009 | 1.27 ± 0.02 | | | |
| | 316 | 1.203 ± 0.037 | 0.58 ± 0.02 | | | |
| **4PF$_6$** | 323 | 0.150 ± 0.003 | 4.63 ± 0.10 | 98.3 ± 14.1 | 95.5 ± 14.1 | −35.1 ± 42.5 |
| | 328 | 0.266 ± 0.007 | 2.61 ± 0.07 | | | |
| | 333 | 0.643 ± 0.016 | 1.08 ± 0.03 | | | |
| | 343 | 1.217 ± 0.039 | 0.57 ± 0.02 | | | |
| **5PF$_6$** | 318 | 0.073 ± 0.001 | 9.45 ± 0.14 | 105.4 ± 9.8 | 102.6 ± 9.8 | −56.9 ± 29.6 |
| | 328 | 0.343 ± 0.006 | 2.02 ± 0.04 | | | |
| | 333 | 0.609 ± 0.012 | 1.14 ± 0.02 | | | |
| | 347 | 2.105 ± 0.125 | 0.33 ± 0.02 | | | |

**Table 4.** p$K_a^*$ and p$K_a$ Values[a] for the Deprotonation of the Coordinated $D_2O$ in Hydrolyzed Complexes **1A**−**5A**

| complex | | p$K_a^*$ | p$K_a$ |
|---|---|---|---|
| [( $\eta^6$-bip)Os(en)$(OD_2)$]$^{2+}$ | **1A** | 6.37[b] | 6.34[b] |
| [($\eta^6$-THA)Os(en)$(OD_2)$]$^{2+}$ | **2A** | 6.36 | 6.33 |
| [($\eta^6$-p-cym)Os(ampy)$(OD_2)$]$^{2+}$ | **3A** | 6.32 | 6.29 |
| [($\eta^6$-p-cym)Os(bipy)$(OD_2)$]$^{2+}$ | **4A** | 5.81 | 5.82 |
| [($\eta^6$-p-cym)Os(phen)$(OD_2)$]$^{2+}$ | **5A** | 5.80 | 5.81 |

[a] p$K_a$ values calculated from p$K_a^*$ according to ref 30. [b] Ref 19.

deprotonation, and consistent with phosphate bound 5′-GMP, [($\eta^6$-bip)Os(en)(5′-GMP-*O*)]. Peak **x** may be the result of a dinuclear complex in which two {($\eta^6$-bip)Os(en)}$^{2+}$ fragments bind to N7 and phosphate of the same 5′-GMP unit.[32]

Solutions of **1BF$_4$** or the Ru$^{II}$ analogue [($\eta^6$-bip)Ru(en)Cl]$PF_6$ **1R** (1 mM to 50 $\mu$M) containing 1 mol equiv 9EtG were incubated at 310 K, and their $^1$H NMR spectra were recorded. Peaks for free 9EtG (H8, 8.10 ppm) increased in intensity with a decrease in metal concentration, Figure S6. Species distribution plots based on peak integrals, Figure 7, yielded apparent formation constants of log $K = 3.13 \pm 0.03$ and 4.78 ± 0.09 for the formation of [($\eta^6$-bip)Os(en)(9EtG)]$^{2+}$ (**1G**) and [($\eta^6$-bip)Ru(en)(9EtG)]$^{2+}$ (**1RG**), respectively.

Similar solutions were prepared by dilution of an equilibrium stock solution of **1BF$_4$** and 9EtG (1 mM) to give 500−50 $\mu$M solutions, which were incubated at 310 K for 24 h before their $^1$H NMR spectra were recorded. Based on $^1$H NMR peak integration of H8 peaks for bound 9EtG (8.21 ppm) and free 9EtG (8.10 ppm), no significant change in ratio occurred with decrease in concentration (Figure S7).

Binding of **1** to 9EtG was further confirmed by ESI-MS. An equilibrium NMR sample (containing equal amounts of **1BF$_4$** and 9EtG), gave peaks at *m*/*z* 294.1 and 585.7 consistent with {($\eta^6$-bip)Os(en)(9EtG)}$^{2+}$ (calcd *m*/*z* 292.6) and {($\eta^6$-bip)Os(en)(9EtG)-H}$^+$ (calcd *m*/*z* 584.2), respectively.

(32) Chen, H.; Parkinson, J. A.; Morris, R. E.; Sadler, P. J. *J. Am. Chem. Soc.* **2003**, *125*, 173−186.

**Table 5.** In Vitro Growth Inhibition of Human A549 Lung and A2780 Ovarian Cancer Cell Lines

| | IC$_{50}$ ($\mu$M) | |
|---|---|---|
| complex | A549 | A2780 |
| **1PF$_6$** | 10 | 7.0 |
| **1BF$_4$** | 10 | 7.6 |
| **2BF$_4$** | 6.4 | 9.4 |
| **3PF$_6$** | >100 | |
| **4PF$_6$** | >100 | |
| **5PF$_6$** | >100 | |
| **6PF$_6$** | *a* | *b* |
| **7PF$_6$** | >100 | |
| **8PF$_6$** | >100 | |
| **9** | >100 | |

[a] <40 $\mu$M, see text. [b] <2 $\mu$M, see text.

**Anticancer Activity.** The cytotoxicity of complexes **1BF$_4$**−**9** toward the human lung A549 cancer cell line and of complexes **1BF$_4$**, **1PF$_6$**, **2BF$_4$**, and **6PF$_6$** toward the human ovarian A2780 cancer cell line was investigated.[33] Complexes **3PF$_6$**−**5PF$_6$** and **7PF$_6$**−**9** were nontoxic up to the highest test concentration (50 $\mu$M). The IC$_{50}$ (concentration inhibiting cell growth by 50%) values are therefore likely to be >100 $\mu$M, and the complexes are deemed inactive. However, complexes **1BF$_4$**, **1PF$_6$**, **2BF$_4$**, and **6PF$_6$** were active (Figure 8 and Table 5). Complexes **1BF$_4$**/**PF$_6$** and **2BF$_4$** displayed IC$_{50}$ values of 6−10 $\mu$M. The IC$_{50}$ values for complex **6PF$_6$** were estimated to be <40 $\mu$M for A549 cells and <2 $\mu$M for A2780 cells. Tests on **6PF$_6$** (as well as **7PF$_6$** and **8PF$_6$**) were complicated by its poor solubility in water. It was initially dissolved in DMSO and then rapidly diluted with water but could only be administered to the cells as a suspension[34] to maintain a low exposure of the cells to DMSO (0.25%).

(33) The IC$_{50}$ values for cisplatin were 2.6 and 0.5 $\mu$M for these human A549 lung and A2780 ovarian cancer cell lines, respectively, as reported previously: S. M. Guichard, R. Else, E. Reid, B. Zeitlin, R. Aird, M. Muir, M. Dodds, H. Fiebig, P. J. Sadler, D. I. Jodrell *Biochem. Pharmacol.* **2006**, *71*, 408−415.

(34) Drugs are sometimes administered as suspensions, although usually in peanut oil and not as a suspension in water as used here. Cells were washed after removal of complex, in an attempt to remove unreacted particles.

**Stability Studies.** Since complex **1BF$_4$** had previously been found to have a low cytotoxicity,[19] its stability during the sample preparation process was investigated. This initially involved dissolution in DMSO and subsequent dilution with water. Solutions of **1BF$_4$** in DMSO were prepared; one sample was stored stoppered at ambient temperature in the dark, and the second sample was exposed to the air, heat, sonication, and light, all of which may have been encountered during the earlier sample preparation. Directly after sample preparation the solution was clear and pale yellow color. After 24 h, the first sample appeared unchanged, and no additional peaks were present in the $^1$H NMR spectrum. However, the second sample (exposed to extreme conditions) was now dark red, and new peaks were seen in the $^1$H NMR spectrum (Figure S8).

$^1$H NMR spectra of 1 mM solutions of the active complexes, **1PF$_6$**/**BF$_4$** and **2BF$_4$** in isotonic saline solution (150 mM NaCl) were recorded directly after sample preparation and after storage at ambient temperature in the dark for 1 week, 2 weeks, and 2 months. Small peaks for the aqua complexes (<10%) were present. The only changes in the $^1$H NMR spectra were loss of peaks assigned as the NH protons of en because of the exchange with deuterium (Figure S9).

The $^1$H NMR spectrum of a 50 $\mu$M solution of **3PF$_6$** in $D_2O$, ~10 min after sample preparation, gave rise to *p*-cymene arene peaks predominantly for the aqua complex **3A** (78%) with minor peaks present for the intact chloro species **3** (12%). No new peaks appeared after incubation of the sample at 310 K for 24 h (Figure S10).

## Discussion

Eight new osmium arene complexes with the general formula $[(\eta^6\text{-arene})Os(NN)Cl]^+$, where NN = bidentate nitrogen-chelating ligands, **1PF$_6$**−**8PF$_6$** and $[(\eta^6\text{-bip})Os(NCCH_3)Cl_2]$ (**9**) were synthesized via the Cl-bridged dimers, $[(\eta^6\text{-arene})OsCl_2]_2$. Complex **1BF$_4$**, $[(\eta^6\text{-bip})Os(en)Cl]BF_4$, had been synthesized previously,[19] but an improved synthesis is reported here.

**X-ray Crystal Structures.** We determined the X-ray crystal structure of the $PF_6^-$ salt of complex **1** for comparison with that of the $BPh_4^-$ salt which we reported previously.[19] They are structurally very similar. The X-ray structure of complex **2BF$_4$** appears to be the first of an osmium complex bound to tetrahydroanthracene (THA). In **2BF$_4$**, the arene, THA, is planar, as it is in the ruthenium analogue of **2**, and it has been proposed that the increase in cytotoxicity of $[(\eta^6\text{-arene})Ru(en)Cl]^+$, on replacing bip with THA may be partly the result of the ability of coordinated THA to intercalate into DNA.[22] The ability of the THA ligand to $\pi-\pi$ stack is evident in the crystal structure of the osmium complex **2BF$_4$**, Figure S1; $\pi-\pi$ stacking is also evident in the crystal structures of complexes **5PF$_6$** and **6PF$_6$**, especially for **6PF$_6$** involving the dppz ligand, which has been extensively studied as a DNA intercalator.[15,35] This feature in combination with the flexible extended arene ring system of bip may mean that intercalation via both dppz and bip can contribute to the cytotoxicity of **6PF$_6$**. Finally, the crystal structures of the highly colored complexes containing azopyridine type ligands in **7PF$_6$** and **8PF$_6$**, also show $\pi-\pi$ stacking. The crystal structure of the ruthenium analogue of **8PF$_6$** has previously been determined and again appears to be structurally similar.[36] These appear to be the first reported X-ray crystal structures of osmium arene complexes, containing coordinated dppz or azopyridine ligands.

**Rates of Hydrolysis and Acidity of Coordinated Water.** The incorporation of a chelating ligand into these $Os^{II}$ arene complexes is crucial for maintaining their aqueous stability. Complex **9**, which contains only monodentate non-arene ligands and a single donor nitrogen ligand, is largely deactivated in water to form predominantly the inert hydroxo-bridged dimer, $[(\eta^6\text{-bip})Os(\mu\text{-OD})_3Os(\eta^6\text{-bip})]^+$ (Figure 4).

The rate of hydrolysis of complex **3**, $[(\eta^6\text{-}p\text{-cym})Os(ampy)Cl]^+$, was found to be markedly pH*-dependent, increasing with increase in pH*. Two equilibria are involved (eq 1), the first of which is hydrolysis and the second is deprotonation of coordinated water. Because of the relatively low $pK_a^*$ values of water coordinated to osmium in these complexes, the hydroxo species is formed even at neutral pH*. This shifts the equilibrium to the right, effectively increasing the rate of hydrolysis. To measure the rate of the hydrolysis step, alone, the pH* was lowered.

$$\{\text{Os-Cl}\}^+ \underset{+\text{Cl}^-}{\overset{+\text{H}_2\text{O}}{\rightleftharpoons}} \{\text{Os-OH}_2\}^{2+} \underset{+\text{H}^+}{\overset{-\text{H}^+}{\rightleftharpoons}} \{\text{Os-OH}\}^+ \qquad (1)$$

The strong dependence of the rate of hydrolysis of **3PF$_6$** on pH*, and the presence of exchangeable NH protons on the chelated ligand, suggest that a conjugate base mechanism may be involved.

The rate of hydrolysis of complexes **1BF$_4$** and **2BF$_4$** containing a chelating ligand with two primary amine donors, en, is faster than that for complexes containing two $\pi$-acceptor pyridine groups, bipy and phen, (~5.5 and 8 times, respectively). This is attributable to the reduced electron density on $Os^{II}$. Intriguingly, complex **3PF$_6$**, which contains the unsymmetrical chelated ligand, 2-picolylamine, hydrolyzed the most rapidly, despite replacement of one of the amine groups with a pyridine. This is contrary to the expected trend and that observed for square-planar platinum complexes.[10] The rate of hydrolysis of complex **3PF$_6$** was also the most sensitive to changes in pH*. A direct comparison between complexes **1BF$_4$**−**2BF$_4$** and **3PF$_6$**−**5PF$_6$** cannot be made because of the different nature of the arenes, with *p*-cymene being more electron-rich than either biphenyl (bip) or tetrahydroanthracene (THA). Complex **2BF$_4$**, containing THA as the arene, hydrolyzed almost twice as fast as complex **1BF$_4$**, in which the arene is bip, in agreement with observations made for the ruthenium analogues.[37]

(35) Frodl, A.; Herebian, D.; Sheldrick, W. S. *J. Chem. Soc., Dalton Trans.* **2002**, *19*, 3664−3673.

(36) Dougan, S. J.; Melchart, M.; Habtemariam, A.; Parsons, S.; Sadler, P. J. *Inorg. Chem.* **2006**, *45*, 10882−10894.

(37) Wang, F.; Chen, H.; Parsons, S.; Oswald, I. D. H.; Davidson, J. E.; Sadler, P. J. *Chem.—Eur. J.* **2003**, *9*, 5810−5820.

Osmium complexes are generally more inert than those of their lighter congener ruthenium, and the data reported here show that complexes **1BF$_4$** and **2BF$_4$** hydrolyze 100 times more slowly than their ruthenium analogues, [($\eta^6$-bip/THA)Ru(en)Cl]$^+$.[37] Hydrolysis of the osmium complex [($\eta^6$-bz)Os(en)Cl]$^+$ and anation of the aqua adduct [($\eta^6$-bz)Os(en)(OH$_2$)]$^{2+}$ have also been reported to occur ~100 times more slowly ($k_{hydro} = 1.2 \times 10^{-5}$ s$^{-1}$ and $k_{Cl} = 0.13 \times 10^{-2}$ M$^{-1}$ s$^{-1}$, 298 K)[38] than for the related ruthenium complexes, [($\eta^6$-bip)Ru(en)(Cl/OH$_2$)]$^{+/2+}$ ($k_{hydro} = 1.3 \times 10^{-3}$ s$^{-1}$ and $k_{Cl} = 0.15$ M$^{-1}$ s$^{-1}$, 298 K).[37] The activation parameters for hydrolysis of the complexes [($\eta^6$-bip)M(en)Cl]$^+$, where M = Os or Ru, can now be compared.[37] As expected the Arrhenius activation energy, $E_a$, for hydrolysis of the osmium complex is higher than that for its ruthenium analogue ($\Delta E_a \approx 26$ kJ mol$^{-1}$) as is the enthalpy of activation, $\Delta H^{\ddagger}$, ($\Delta\Delta H^{\ddagger} \approx 26$ kJ mol$^{-1}$) with similar entropies of activation, $\Delta S^{\ddagger}$. The $\Delta E_a$ of 26 kJ mol$^{-1}$ is in good agreement with reported theoretical calculations, which give a $\Delta E_a$ value of 20 kJ mol$^{-1}$ for the hydrolysis of these Os$^{II}$ and Ru$^{II}$ complexes.[20,39] The large negative $\Delta S^{\ddagger}$ values for the hydrolysis of osmium complexes **1BF$_4$**−**3PF$_6$** are indicative of an associative process (Table 3). The errors associated with the $\Delta S^{\ddagger}$ values for the hydrolysis of complexes **4PF$_6$** and **5PF$_6$** are too large to allow comparisons.

Another indication of the electron density on osmium and of the Os−O bond strength, is the acidity of the coordinated water. When the p$K_a^*$ values of the aqua complexes **1A**, **2A**, **3A**, **4A**, and **5A** (Table 4) are compared, it is evident that water coordinated to osmium bound to two $\pi$-acceptor groups such as pyridines is more acidic (p$K_a^* = 5.8$) than when one of the nitrogen donors is a primary amine (p$K_a^* = 6.3$). Water bound to ruthenium analogues is less acidic but shows the same trend: p$K_a$ values of 7.71 and 7.2 for [($\eta^6$-bip)Ru(en)(OH$_2$)]$^{2+}$ and [($\eta^6$-*p*-cym)Ru(bipy)(OH$_2$)]$^{2+}$, respectively.[37,40]

**Binding to Guanine.** The kinetics for the reactions of **3PF$_6$** and **1BF$_4$** with 9EtG and 5′-GMP, respectively, were investigated. In addition, the stability constants of [($\eta^6$-bip)Os(en)(9EtG)]$^{2+}$ **1G** and its ruthenium analogue [($\eta^6$-bip)Ru(en)(9EtG)]$^{2+}$ **1RG** were determined.

The reaction of the bip/en complex **1BF$_4$** with 5′-GMP at 298 K resulted in the formation of three Os$^{II}$−GMP adducts (2 major and 1 very minor) as judged by the H8 $^1$H NMR signals. From reported work on the binding of the ruthenium analogue [($\eta^6$-bip)Ru(en)Cl]PF$_6$ **1R** to 5′-GMP[32] and from pH* titrations of the products, the major species can be assigned as N7-bound 5′-GMP, [($\eta^6$-bip)Os(en)(5′-GMP-*N7*)], with the phosphate-bound 5′-GMP adduct [($\eta^6$-bip)Os(en)(5′-GMP-*OP*)] also being formed in significant amounts (ratio of 2:1 for N7/phosphate-bound adducts, after 30 h at 298 K). The minor product (labeled **x** in Figure 6) may be a dinuclear adduct, with two osmium units bound to the nucleotide, one to the N7 and the other to the phosphate group, [($\eta^6$-bip)Os(en)(*OP*-5′-GMP-*N7*)Os(en)($\eta^6$-bip)]$^{2+}$; however its concentration was too low to follow by $^1$H NMR in the pH* titration of the reaction mixture. The time dependence of the species distribution (Figure 6B) within the first 5 h suggests that phosphate binding occurs first, followed by N7 binding. This would be consistent with the migration mechanism proposed by Chen et al.[32] for the ruthenium analogue **1R**. The migration of Os$^{II}$ from the phosphate to N7 of 5′-GMP appears to be slower than that for the ruthenium analog. After 22 h at 298 K, all of the Ru$^{II}$ was bound to the N7 of 5′-GMP,[32] compared to 66% of the bound GMP for Os$^{II}$ (Figure 6B).

The binding constant for formation of the Os$^{II}$ adduct with 9EtG [($\eta^6$- bip)Os(en)(9EtG)]$^+$ (**1G**) of log $K = 3.13 \pm 0.03$ is an order of magnitude lower than that for the Ru$^{II}$ analog (log $K = 4.78 \pm 0.09$), Figure 7. Intriguingly, the stronger binding to Ru(II) is opposite to that observed for the maltolate (mal) complexes [($\eta^6$-*p*-cym)M(mal)(9EtG)]$^+$, for which log $K = 4.41$ (Os) and 3.87 (Ru).[20] Despite the lower formation constant compared to Ru$^{II}$, the kinetic stability of the Os$^{II}$ complex **1G** is high: 9EtG did not readily dissociate, even in 50 $\mu$M solutions incubated at 310 K for 24 h. This suggests that once formed on DNA (or RNA), {($\eta^6$-bip)Os(en)}$^{2+}$ adducts with G bases may persist long enough to interfere with downstream DNA processing (including protein recognition and excision/repair).

**Cancer Cell Cytotoxicity.** We reported previously that complex **1BF$_4$**, [($\eta^6$-bip)Os(en)Cl]BF$_4$, was inactive against the human ovarian A2780 cancer cell line (IC$_{50}$ >100 $\mu$M).[19] Because the chemical properties of the complex (rate of hydrolysis and binding to guanine) appeared to be compatible with activity, we reinvestigated its cytotoxicity. Apart from the potential variability of cell culture media (especially fetal calf serum) and the cell population, a possible explanation of the previous finding of inactivity (IC$_{50}$ > 100 $\mu$M) and the present finding of activity can be related to partial decomposition of the complex in stock solutions prepared in DMSO. We have shown here that solutions of **1BF$_4$** in DMSO can decompose after sonication, heating, and a longer term of standing in air and direct sunlight, as is evident from color change from yellow to dark red (Figure S8A/B). However, such solutions are stable when stoppered and stored at ambient temperature in the dark, and then exhibit good activity, as does the PF$_6$ salt (**1PF$_6$**), giving IC$_{50}$ values of 7−10 $\mu$M against the human ovarian A2780 and lung A549 cancer cell lines (Table 5). The change of the arene from biphenyl in **1BF$_4$** to the extended tetrahydroanthracene gave rise to a similar potency (complex **2BF$_4$**, IC$_{50}$ values of 6−9 $\mu$M, Table 5), whereas for the ruthenium analogues this change in arene increases the activity by 10-fold.[41] Further work will be required to investigate whether Os-bound extended arenes can intercalate into DNA in a manner similar to Ru-bound arenes.[42]

(38) Hung, Y.; Kung, W.; Taube, H. *Inorg. Chem.* **1981**, *20*, 457−463.
(39) Wang, F.; Habtemariam, A.; Geer, E. P. L. v. d.; Fernandez, R.; Melchart, M.; Deeth, R. J.; Aird, R.; Guichard, S.; Fabbiani, F. P. A.; Lozano-Casal, P.; Oswald, I. D. H.; Jodrell, D. I.; Parsons, S.; Sadler, P. J. *Proc. Natl. Acad. Sci. U.S.A.* **2005**, *102*, 18269−18274.
(40) Dadci, L.; Elias, H.; Frey, U.; Hornig, A.; Koelle, U.; Merbach, A. E.; Paulus, H.; Schneider, J. S. *Inorg. Chem.* **1995**, *34*, 306−315.
(41) Aird, R. E.; Cummings, J.; Ritchie, A. A.; Muir, M.; Morris, R. E.; Chen, H.; Sadler, P. J.; Jodrell, D. I. *Br. J. Cancer* **2002**, *86*, 1652−1657.

The *p*-cym/ampy complex **3PF$_6$** was non-cytotoxic toward A549 cells despite its similar rate of hydrolysis to the bip/en and *p*-cym/en complexes **1PF$_6$/BF$_4$** and **2BF$_4$**, stability at micromolar concentrations (50 $\mu$M), and the ability to react with 9EtG under biologically relevant conditions with an associated half-life of 3.2 h. The reasons for the inactivity are therefore not clear. However the other complexes tested which have pyridyl ligands (**4PF$_6$** and **5PF$_6$**) were also inactive, as are some of the Ru$^{II}$ arenes with unsubstituted pyridyl ligands.[43]

The inactivity of complexes **4PF$_6$**, **5PF$_6$**, **7PF$_6$**, and **8PF$_6$** can be correlated with their slow kinetics of hydrolysis and higher acidity of coordinated water. Complex **9**, which contains only monodentate non-arene ligands, is deactivated in water by formation of the inert hydroxo-bridged dimer. The dppz complex **6PF$_6$** is probably too substitution-inert to bind effectively to G bases on DNA, but both the arene (bip) and chelating ligand (dppz) have the ability to intercalate into DNA[15,35] (vide supra), which may contribute to the mechanism of cytotoxicity of **6PF$_6$** against both the A549 and A2780 cancer cell lines.

Despite the instability of complex **1BF$_4$** in DMSO, solutions of the active complexes **1PF$_6$/BF$_4$** and **2BF$_4$** were found to be stable in isotonic saline solutions (150 mM NaCl) stored at ambient temperature in the dark over a period of 2 months. This suggests that drug formulation in aqueous solution would be feasible for these complexes.

## Conclusions

Although organometallic complexes offer a versatile platform for the design of new medicines, and of anticancer agents in particular, their aqueous solution chemistry has been relatively little explored. An understanding of how ligand design can be used to control their redox and ligand substitution reactions under conditions of biological relevance is vital for the establishment of structure−activity relationships and for understanding their mechanisms of action.

Although osmium complexes are often considered to be kinetically inert, we have shown that the reactivity of half-sandwich Os$^{II}$ arene complexes depends strongly on the other ligands in the complex, which can play both steric and electronic roles. Here we have shown that although [($\eta^6$-arene)Os(N,N)Cl]$^+$ complexes containing en as the N,N-chelator hydrolyze relatively rapidly ($t_{1/2}$ = 1.6 h at 310 K for complex **2BF$_4$**), the introduction of $\pi$-acceptor pyridines as the N-donors, considerably slows down hydrolysis (e.g., by an order of magnitude for complex **5PF$_6$**), and a large window of reactivity can therefore be accessed. The introduction of an $\pi$-acceptor N-donor also increases the acidity of the aqua adduct. The en complexes [($\eta^6$-bip)Os(en)Cl]-PF$_6$/BF$_4$ and [($\eta^6$-THA)Os(en)Cl]BF$_4$ are as cytotoxic to human A549 lung and A2780 ovarian cancer cells as the drug carboplatin, whereas those complexes containing a pyridine N-donor were inactive. An exception is the dppz complex with biphenyl as the arene [($\eta^6$-bip)Os(dppz)Cl]-PF$_6$ (**6PF$_6$**), which can also act as a DNA intercalator.

Although {($\eta^6$-bip)Os(en)}$^{2+}$ adducts with G nucleobases appear to be less thermodynamically stable than similar adducts thought to be responsible for the anticancer activity of the Ru$^{II}$ analogues, once formed the Os$^{II}$ adducts have some kinetic stability with respect to dissociation. It is unclear why the complex [($\eta^6$-*p*-cym)Os(ampy)Cl]PF$_6$ (**3PF$_6$**) exhibits low cytotoxicity, since it hydrolyzes at a similar rate, has a similar p$K_a^*$ for its aqua adduct, and a similar rate of binding to G nucleobases as the active complexes **1PF$_6$/BF$_4$** and **2BF$_4$**.

Thus we have shown that half-sandwich Os$^{II}$ arene complexes containing N,N-chelating ligands can be designed which have cancer cell cytotoxicity comparable to their Ru$^{II}$ analogs, but the reactivities are 100 times less. Such a range of kinetic effects can be useful for balancing cytotoxicity and unwanted side-effects of anticancer drugs, as illustrated by the clinical profiles of cisplatin and the less-labile second generation drug carboplatin. Some of the Os$^{II}$ complexes prepared here appear to be stable under conditions relevant to drug formulation (e.g., isotonic saline) and are interesting candidates for further investigation.

**Acknowledgment.** We thank the EPSRC and The University of Edinburgh (studentship for A.F.A.P.), Dr. Michael Melchart (Edinburgh) for the gift of the dppz ligand, Rhona E. Aird and Professor Duncan Jodrell (Western General Hospital/Cancer Research U.K. Centre) for advice and assistance with cell culture, and members of EC COST groups D20 and D39 for stimulating discussions.

**Supporting Information Available:** Details of the crystallographic data (Figures S1−S3), aqueous and nucleobase binding studies (Figures S4−S7) and stability studies (Figure S8−S10), and X-ray crystallographic data in CIF format. This material is available free of charge via the Internet at http://pubs.acs.org.

IC062350D

(42) Liu, H.-K.; Berners-Price, S. J.; Wang, F.; Parkinson, J. A.; Xu, J.; Bella, J.; Sadler, P. J. *Angew. Chem., Int. Ed.* **2006**, *45*, 8153−8156.
(43) Habtemariam, A.; Melchart, M.; Fernández, R.; Parsons, S.; Oswald, I.; Parkin, A.; Fabbiani, F. P. A.; Davidson, J.; Dawson, A.; Aird, R. E.; Jodrell, D. I.; Sadler, P. J. *J. Med. Chem.* **2006**, *49*, 6858−6868.